Three-component Synthesis of Electron-poor Alkenes using Isatin Derivatives, Acetylenic Esters, Triphenylphosphine and Theoretical Study

Masoome Sheikhi,[a,*] Davood Sheikh[b] and Ali Ramazani[c]

[a]*Young Researchers & Elite Club, Gorgan Branch, Islamic Azad University, Gorgan, Iran.*
[b]*Young Researchers & Elite Club, Hamedan Branch, Islamic Azad University, Hamedan, Iran.*
[c]*Department of Chemistry, University of Zanjan, Zanjan, Iran.*

Received 13 July 2014, revised 23 September 2014, accepted 24 September 2014.

ABSTRACT

Synthesis of electron-poor alkenes has been reported by 1,2-proton shift and elimination of triphenyl phosphine from phosphorus ylide in good to high yields. The structures of six novel products were deduced from their IR, ^{1}H NMR, and ^{13}C NMR spectra. The B3LYP/HF calculations for computation of ^{1}H and ^{13}C NMR chemical shifts have been carried out for the compounds with the 6-31G* basis set utilizing the GIAO approach. In addition, theoretical configurations of the title compound were studied in terms of the combined analysis of the HOMO–LUMO energy gap, NBO analysis, thermodynamic parameters and molecular electrostatic potential (MEP). Also ionization potential (*I*), electron affinity (*A*), chemical hardness (η), electronic chemical potential (μ) and electrophilicity (ω) of the title molecule are reported. All calculations were performed using B3LYP method with the 6-31G* basis set.

KEYWORDS

Isatin, electron-poor alkenes, DFT, NBO, HOMO, LUMO.

1. Introduction

The development of new stereoselective reactions has been a major topic in synthetic organic chemistry.[1–3] Organophosphorus compounds have been used in organic synthesis as useful reagents as well as ligands of a number of transition metal catalysts.[4]

Acetylenic esters are reactive systems taking part in many chemical synthesis, for example, as Michael acceptors.[5] In recent years, there has been increasing interest in the application of acetylenic esters for multi-component synthesis.[6–9] Multi-component reactions (MCRs) have proved to be notably successful in generating products in a single synthetic operation.[10–11] The development of new MCRs and improvement of known multi-component reactions are the subjects of considerable current interest.

Acrylic compounds are good Michael acceptors due to their great reactivity as electrophiles towards nucleophiles, particularly in the preparation of natural and biologically active compounds.[12–15] Acrylates form a versatile class of polymers that play a major role in military and commercial products.[16] Compounds with alkyl acrylate skeletons have significant importance in material science.[17]

* To whom correspondence should be addressed. E-mail: m.sheikhi2@gmail.com

Because of their wide range of industrial and synthetic applications, substituted acrylates have recently received a great deal of attention.[18–20] Therefore, in this paper, we present a simple, mild and efficient synthesis of these compounds in good yields (Scheme 1).

In recent years, computational chemistry has become an important tool for chemists and a well-accepted partner for experimental chemistry.[21–26] Density functional theory (DFT) and Hartree-Fock (HF) methods have become a major tool in the methodological arsenal of computational organic chemists. Recently, the GIAO (gauge including atomic orbitals) method for the calculation of NMR chemical shifts have been implemented in major quantum chemistry packages.[27–29] The GIAO approach facilitates accurate NMR shift calculations *via* electron-correlated methods. In this paper we will discuss the accuracy of the calculation of ^{1}H and ^{13}C chemical shifts performed at both the HF and density functional theory (B3LYP) frameworks using the GIAO technique with the 6- 31G* basis set.

2. Results and Discussion

On the basis of the well established chemistry of trivalent phosphorus nucleophiles,[22,30] it is reasonable to assume that phosphorus ylides **6** result from the initial addition of triphenyl-

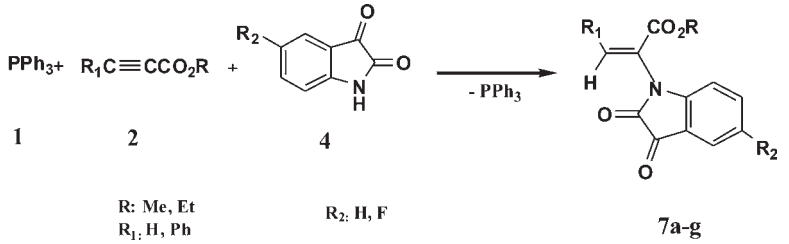

Scheme 1

Three-component reaction of triphenylphosohine **1**, acetylenic esters **2** and isatin derivatives **4**.

phosphine to the acetylenic ester and protonation of the 1:1 adduct by isatin derivatives, then the positively charged ion is attacked by the isatin anion. The scope of the reaction was extended to a variety of structurally diverse acetylenic esters. All the reactions proceeded smoothly to provide the corresponding new products **7a–g** in satisfactory yields and the results are summarized in Table 1. Compounds **7a, 7b, 7c, 7e** and **7g** are stable solid powders. IR, ^{1}H NMR and ^{13}C NMR data are useful information for the structural assignment of the products. We isolated **7a** and **7b** as a mixure of diastereomers, which were then separated with column chromotography. The ^{1}H NMR ($CDCl_3$) spectra of the crude product (mixture: **7a** and **7b)** show the presence of two stereoisomers (**7a**: **E** and **7b**: **Z**).[31] Also the ^{1}H NMR spectra show that the two stereoisomers (**E** and **Z**) are not in equilibrium (**E**/**Z**: 46/54). The relative population of **E** and **Z** isomers were determined *via* their ^{1}H NMR spectra (based on reported relative intensities of the olefinic protons of **E** and **Z** isomers (=CH)).[31,32] Also, product **7e** was isolated as one stereoisomer **Z**. The ^{1}H NMR spectrum of **7a, 7b** and **7e** exhibited one singlet line at 5.29, 8.11 and 8.10 ppm for the =CH group.

Table 1 Synthesis of new electron-poor alkenes **7a–g**.[a]

Entry	Acetylenic esters	Product	Time/min	Yield/%[b]
a	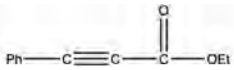	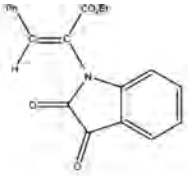	15	46
b		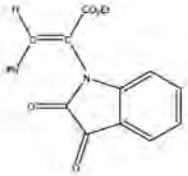	15	54
c	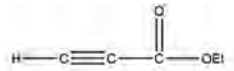	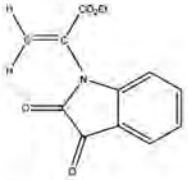	15	85
d	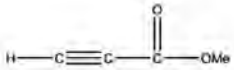	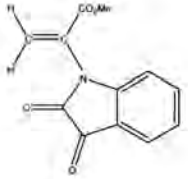	2 (days)	80
e	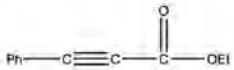	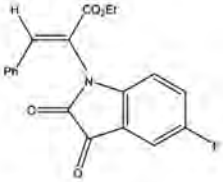	2 (days)	90
f	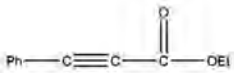	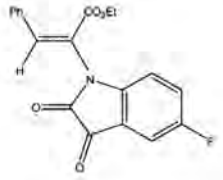	2 (days)	0
g	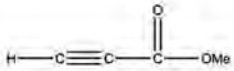	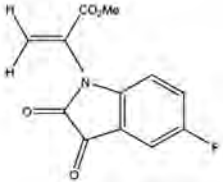	2 (days)	95

[a] Conditions: triphenylphosphine (1 mmol), isatin derivatives (1 mmol), acetylenic esters (1 mmol), dry dichloromethane (9 mL).
[b] Isolated yields.

Further confirmation of the structures was obtained from the ^{13}C NMR spectra which displayed olefinic carbon (=CH) resonances of **7a**, **7b** and **7e** at about 132.5, 131.6 and 131.5, respectively, and carbonyl carbons at about δ = 158–183 (see Experimental section).[32] The shift at 8.11 ppm of the =CH group of the **Z** rotamers (**7b** and **7e**) is deshielded. Also the ^{1}H NMR spectrum of **7c, 7d** and **7g** displayed signals for =CH_2 protons as two sets of singlets at δ = 6.09, 7.26, δ = 7.26, 7.69 and δ = 7.54, 7.62 ppm, respectively.

The theoretical results of NMR calculations of the structures correspond with the experimental data (see Theoretical section, Tables 2 and 3). This supports the proposed structures.

A possible mechanism to explain the formation of the products **7a–g** is depicted in Scheme 2. The formation of products **7a–g** can be rationalized by initial formation of intermediates **3** through the standard Michael addition of the triphenylphosphine **1** to the β-carbon of the electron-deficient alkyne **2**. Protonation of **3** by isatin derivatives **4** leads to vinyltriphenylphosphonium salts **5**, which undergoes a Michael addition reaction with conjugated base to produce phosphorus ylides **6**. The ylides are converted to products **7a–g** *via* elimination of triphenylphosphine under the correct reaction conditions.

2.1. ^{1}H and ^{13}C NMR Chemical Shifts

In the present work, we have calculated the ^{1}H and ^{13}C NMR chemical shifts using HF/B3LYP methods with the 6-31G* basis set and the GIAO approach for compounds **7a–g**. The theoretical geometric structure of **7a** is shown in Fig. 1. The observed ^{1}H and ^{13}C NMR chemical shifts and the calculated values are presented in Tables 2 and 3, respectively.

The theoretical ^{1}H NMR data of **7a, 7b** and **7e** exhibited one singlet at 5.9, 8.2 and 8.21 ppm for the =CH group (B3LYP/6-31G*). Also, the theoretical ^{13}C NMR for the olefinic carbon (=CH) of **7a**, **7b** and **7e** are displayed at about 133.6, 130.8 and 131.4, respectively (B3LYP/6-31G*).

The theoretical calculations were performed for the diastereomeric alkene of **7e** (isomer **7f**, which was isolated in trace amounts, see Tables 2 and 3). The theoretical ^{1}H NMR data of **7f** exhibited one singlet at 5.7 ppm for the =CH group (B3LYP/6-31G*). Also, the theoretical ^{13}C NMR for the olefinic carbon (=CH) of this alkene is displayed at about 133.4 (B3LYP/6-31G*, see Tables 2 and 3). Both the proton and ^{13}C NMR deviate considerably from the experimentally observed signals for **7e**, confirming the correct assignment thereof.

On the basis of our calculations and experimental ^{1}H and ^{13}C NMR chemical shifts, we observed excellent agreement between the experimental and theoretical results. This confirms our initial NMR assignments for these compounds. In order to compare this agreement, the correlation graphic based on the theoretical and experimental data was investigated. The correlation value (R^2) of molecule **7a** for HF/6-31G* and B3LYP/6-31G* is 0.99 and 0.9995, respectively (Fig. 2).

Table 2 Experimentally measured and calculated (HF/6-31G* and B3LYP/6-31G*)[a] ^{1}H chemical shifts δ (ppm, *vs*. TMS) of molecules **7a–g**.

	H atom	Exp.	HF/6-31G* GIAO	B3LYP/6-31G* GIAO
7a	3H, CH_3	1.1	1.3	1.3
	2H, OCH_2	4.2	4	4.5
	H aromatic	7.1–7.7	6.9–7.9	7.3–7.5
	= CH	5.3	6.61	5.9
7b	3H, CH_3	1.3	1	1.1
	2H, OCH_2	4.3	3.6	4.4
	= CH	8.1	8.5	8.2
	H aromatic	6.6–8	6.3–8	6.5–8.3
7c	3H, CH_3	1.3	1	1.5
	2H, OCH_2	4.8	4	4.5
	2H, =CH_2	6.1,7.3	6.2,7.2	6.2,7.2
	H aromatic	6.7–7.7	6.5–8.1	6.8–7.8
7d	3H, CH_3	4.2	3.5	4.1
	2H, =CH2	7.2,7.7	6.9,7.2	7,7.2
	H aromatic	7.5–7.7	7.1–8.1	7–7.9
7e	3H, CH_3	1.3	1	1.31
	2H, OCH_2	4.3	4	4.5
	1H, = CH	8.1	8.5	8.21
	H aromatic	7.1–7.6	6.9–7.9	6.6–8.3
7f[b]	3H, CH_3	–	1.2	1.34
	2H, OCH_2	–	4.4	4.1
	1H, = CH	–	6.1	5.7
	H aromatic	–	7.2–8	7–7.5
7g	3H, CH_3	3.5	3.4	3.4
	2H, = CH_2	7.5,7.5	7.1,7.2	6.2,7.2
	H aromatic	7.4–7.8	7.1–7.7	6.7–7.5

[a] The Cartesian coordinates of the 3D structures for all these compounds are provided with the supplementary material.
[b] **7f** is the alternative diastereomeric product of **7e**, which was only isolated in trace amounts.

Table 3 Experimentally measured and calculated (HF/6-31G* and B3LYP/6-31G*)[a] ^{13}C chemical shifts δ (ppm, *vs*. TMS) of molecules **7a–g**.

	H atom	Exp.	HF/6-31G* GIAO	B3LYP/6-31G* GIAO
7a	OCH_2	62.2	59	65
	=CH	132.5	136	133.6
	C=O amide	158	152	160
	C=O ester	163	155	165
	C=O ketone	182.4	172.9	186.4
7b	OCH_2	62.3	59.8	60.2
	=CH	131.6	131.5	130.8
	C=O amide	158	154.2	161.5
	C=O ester	163	156	165.7
	C=O ketone	181.9	172.7	185.2
7c	OCH_2	62.3	59.9	63.5
	=CH	128.6	118.6	120
	C=O amide	161.6	158.7	160.0
	C=O ester	161.7	160.5	164.8
	C=O ketone	183.4	172.5	185.6
7d	= CH	128.3	119.1	120.1
	C=O amide	159	151.5	157.5
	C=O ester	162	160.7	164.2
	C=O ketone	181.9	172.5	184.6
7e	OCH_2	62.3	53	55
	= CH	131.5	131.8	131.4
	C=O amide	162.8	159.7	161.4
	C=O ester	162.8	155.8	160.5
7f[b]	OCH_2	–	59.8	63.4
	= CH	–	134.8	133.4
	C=O amide	–	161.2	159.5
	C=O ester	–	159	162.4
7g	=CH	128.4	120	120.4
	C=O amide	158	151.2	157.6
	C=O ester	163	160.5	164.1
	C=O ketone	181.9	172.1	184.1

[a] The Cartesian coordinates of the 3D structures for all these compounds are provided with the supplementary material.
[b] **7f** is the alternative diastereomeric product of **7e**, which was only isolated in trace amounts.

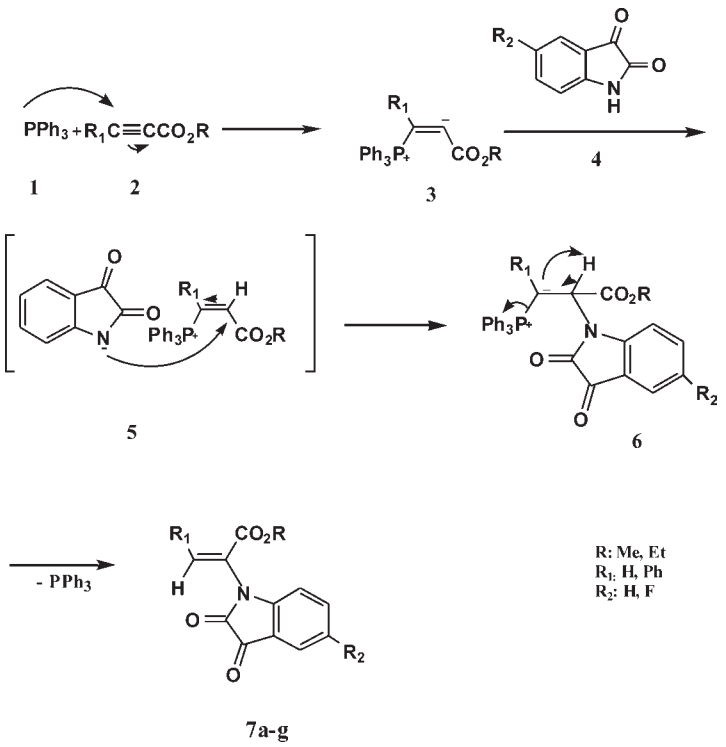

Scheme 2
General mechanism for synthesis electron-poor alkenes.

2.2. Thermodynamic Analysis

Thermodynamic analysis indicates that the relative energies (ΔE), enthalpies (ΔH) and Gibbs free energy (ΔG) are negative for molecules **7a–g** whereas the calculated entropies (ΔS) are positive. This indicates that these molecules are stable in the gas phase (see Table 4).

Dipole moment is a good measure for the asymmetric nature of a molecule. The values of dipole moment for molecules **7a–g** are listed in Table 5. The size of the dipole moment depends on the composition and dimensionality of the 3D structures. All structures have relative high dipole moment values. All the structures have the C1 point group, which refers to high asymmetry of the structure. As can be seen, the dipole moment for structure of **7b** is relatively high (B3LYP/6-31G* = 5.8233 Debye). The high value of dipole moment for **7b** is due to its asymmetric character. Since product **7b** is the **Z** isomer, the atoms are irregularly arranged which gives rise to the increased dipole moment (with respect to **7a** at 4.94 Debye).

In order to study the atomic charge distribution of compound **7a**, the natural bond orbital charges (NBO) have been calculated and are presented in Fig. 3. As seen in Fig. 3, the atomic charge distribution is different. As expected, the O_{10}, O_{11}, O_{16} and O_{17} atoms have negative charges (–0.529e, –0.480e, –0.547e and –0.612e, respectively) whereas all the hydrogen atoms carry positive charge. The N_7 atom has a large negative charge (–0.469e). All carbon atoms of phenyl ring exhibit nega-

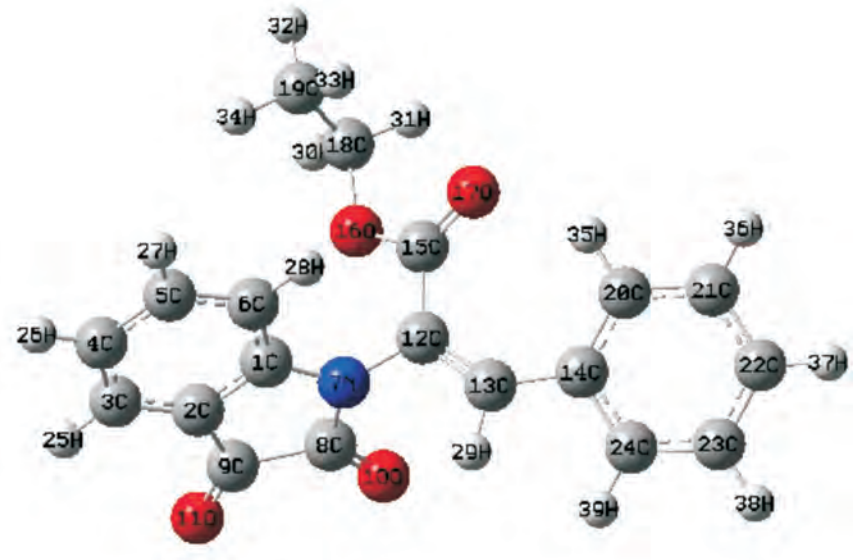

Figure 1 Theoretical geometric structure of **7a** optimized with B3LYP/6-31G* in vacuum (the Cartesian coordinates of the 3D structure are provided with the supplementary material).

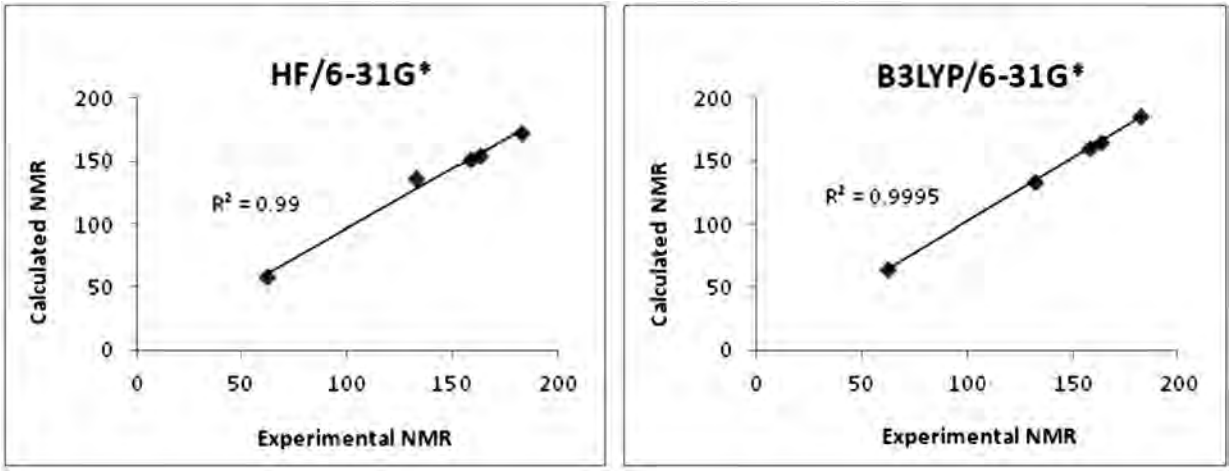

Figure 2 Correlation graphic of calculated and experimental ^{13}C chemical shifts for **7a** with HF/6-31G* and B3LYP/6-31G* using the GIAO approach.

Table 4 Relative thermochemical parameters of structurea **7a–g** [a] obtained in gas phase using two levels of theory.

	Level	ΔE/kcal mol^{-1}	ΔG/kcal mol^{-1}	ΔH/kcal mol^{-1}	ΔS/kcal mol^{-1}	Cv/kcal mol^{-1}
7a	HF/6-31G*	–678841.8108	–678886.5906	–678841.2185	152.180	72.261
	B3LYP /6-31G*	–683170.9832	–683214.6715	–683170.3186	159.203	76.165
7b	HF/6-31G*	–678847.8651	–678892.1967	–678847.2727	150.6767	2.245
	B3LYP /6-31G*	–683174.7969	–683306.422	–683174.2510	158.397	76.118
7c	HF/6-31G*	–534858.4270	–534896.0795	–534857.8340	128.275	55.259
	B3LYP /6-31G*	–538034.0022	–538072.4541	538033.4098	130.955	59.612
7d	HF/6-31G*	–510380.1060	–510415.6431	–510379.5136	121.179	50.682
	B3LYP /6-31G*	–513379.4633	–513415.6957	–513378.8709	123.511	54.731
7e	HF/6-31G*	–740880.1749	–740925.7716	–740879.5825	154.920	75.216
	B3LYP /6-31G*	–745258.6864	–745290.1664	–745244.5380	161.005	81.119
7f [b]	HF/6-31G*	–740698.3165	–740765.8224	–740690.7243	157.023	76.291
	B3LYP /6-31G*	–743596.6859	–743634.3157	–743581.7265	163.241	84.694
7g	HF/6-31G*	–572412.2909	–572449.0611	–572411.6980	125.315	53.652
	B3LYP /6-31G*	–575652.0189	–575689.6927	–575651.4265	128.345	57.797

[a] The Cartesian coordinates of the 3D structures for all these compounds are provided with the supplementary material.
[b] **7f** is the alternative diastereomeric product of **7e**, which was only isolated in trace amounts.

Table 5 Calculated (B3LYP/6-31G* and HF/6-31G*) dipole moment and point group of structure of **7a–g** obtained in gas phase using two levels.

	7a	**7b**	**7c**	**7d**	**7e**	**7f**	**7g**
HF/6-31G*	5.3531	5.8575	5.7990	5.8741	4.8369	4.2964	4.8009
B3LYP /6-31G*	4.9420	5.8233	5.2768	5.2230	5.0333	4.08731	4.4056
Point group	C1	C1	C1	C1	C1	C1	C1

tive charges. The C_8, C_9 and C_{15} (carbon of carbonyl groups) have more positive charge (0.635e, 0.485e and 0.795e, respectively), as is expected. These data clearly show that ester carbonyl carbon (C_{15}) is the most reactive electrophilic atom.

2.3. NBO Analysis

Natural bond orbital analysis is an important method for studying intra- and inter-molecular bonding and interaction between bonds. The results of natural bond orbital (NBO) analysis and the polarization coefficient values of atoms for molecule **7a** are listed in Table 6. According to Table 6, the calculated bonding orbital for the C_1-N_7 bond is BD = 0.6179 $sp^{2.68}$ + 0.7862 $sp^{2.04}$. The polarization coefficients of C_1 = 0.6179 and N_7 = 0.7862 suggest that N_7 is more electron-rich than the C_1 atom. The bonding orbital for the N_7-C_8 bond is BD= 0.8033 $sp^{2.12}$ + 0.5956 $sp^{2.19}$. These polarization coefficients (N_7 0.8033 and C_8 0.5956), also suggest that N_7 is more electron-rich than the C_8 atom. The calculated natural charge (NBO) of the N_7 atom is negative (–0.469e) whereas C_8 has a positive value (0.635e). The bonding orbital of the C_{12}-C_{15} is BD = 0.7204 $sp^{2.05}$ + 0.6935 $sp^{1.62}$. These polarization coefficient (C_{12} 0.7204 and C_{15} 0.6935) suggest that C_{12} is more electron-rich. The calculated natural charge (NBO) of C_{15} atom is more positive (0.795e) than C_{12} atom (0.029e). Thus more charge density resides on C_{12}. For all the C-O bonds, the polarization coefficient value of oxygen atom is greater than the C atom (see Table 6), as expected.

Electron donor orbital, acceptor orbital and the interacting stabilization energy resulting from the second-order micro disturbance theory[33,34] are reported in Table 7. The electron delocalization from filled NBOs (donors) to the empty NBOs

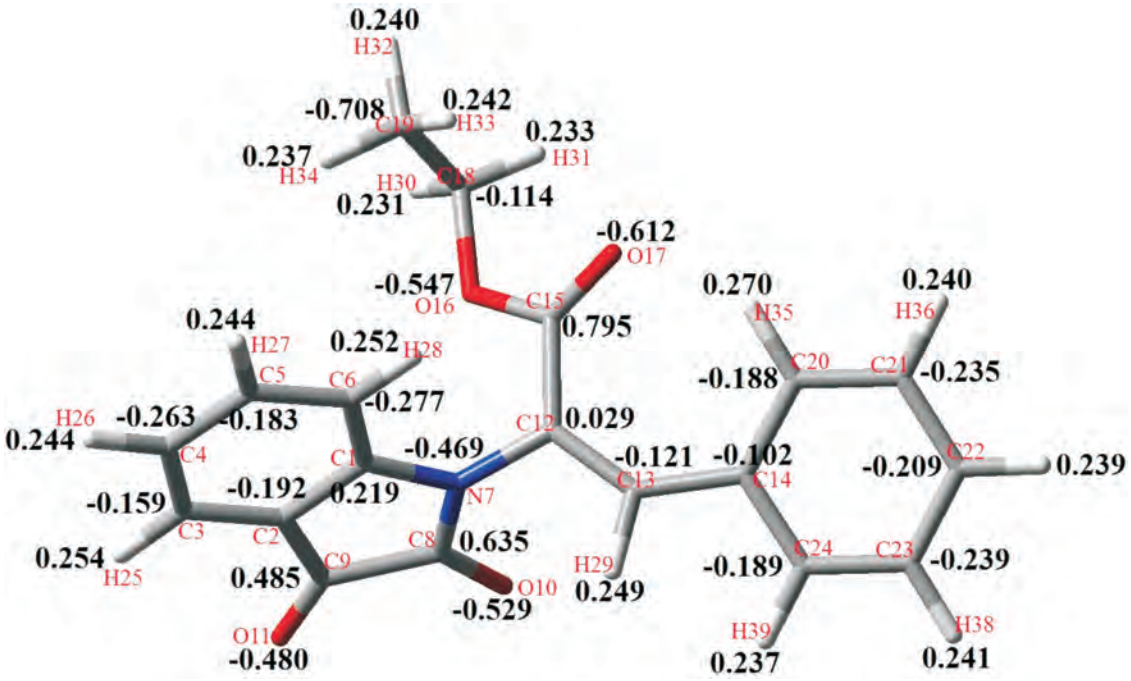

Figure 3 Calculated (B3LYP/6-31G*) natural charges (NBO) of the atoms of molecule **7a**. (The Cartesian coordinates of the optimized structure is available with the supplementary material.).

Table 6 Calculated (B3LYP/6-31G*) natural bond orbitals (NBO) and the polarization coefficient (BD: bonding orbital) for each hybrid in bonds of molecule **7a**.

A-B [a]	A	B
C_1-N_7	$sp^{2.68}$ (0.6179)	$sp^{2.04}$ (0.7862)
C_6-H_{28}	$sp^{2.26}$ (0.7917)	s (0.6109)
N_7-C_8	$sp^{2.12}$ (0.8033)	$sp^{2.19}$ (0.5956)
N_7-C_{12}	$sp^{1.88}$ (0.7920)	$sp^{2.75}$ (0.6105)
C_8-C_9	$sp^{1.93}$ (0.7119)	$sp^{2.34}$ (0.7023)
C_8-O_{10}	$sp^{1.89}$ (0.5881)	$sp^{1.35}d^{0.01}$ (0.8088)
C_9-O_{11}	$sp^{2.04}$ (0.5873)	$sp^{1.33}d^{0.01}$ (0.8093)
C_{12}-C_{13}	$sp^{1.46}$ (0.7101)	$sp^{1.62}$ (0.7041)
C_{12}-C_{15}	$sp^{2.05}$ (0.7204)	$sp^{1.62}$ (0.6935)
C_{13}-C_{14}	$sp^{1.79}$ (0.7063)	$sp^{2.13}$ (0.7079)
C_{13}-H_{29}	$sp^{2.86}$ (0.7889)	s (0.6145)
C_{15}-O_{16}	$sp^{2.58}d^{0.01}$ (0.5590)	$sp^{2.05}$ (0.8292)

[a] A-B is the bond between atom A and atom B. (A: natural bond orbital and the polarization coefficient of atom; A-B: natural bond orbital and the polarization coefficient of atom B).

(acceptors) describes a conjugative electron transfer process between them. For each donor (*i*) and acceptor (*j*), the stabilization energy $E^{(2)}$ associated with the delocalization $i \rightarrow j$ is estimated. The resonance energy ($E^{(2)}$) shows the amount of participation of electrons in expected the resonance between atoms. According to the results of the NBO analysis for molecule **7a** (Table 7), the greatest resonance energy ($E^{(2)}$) is 50.87 for LP(1)N_7 that participates as donor and C_8-O_{10} [anti-bonding BD*(2)] as acceptor. These results suggest that charge is transferred from N_7 to C_8-O_{10} ($N_7 \rightarrow C_8$-O_{10}). The calculated natural charge of N_7 (–0.469e) and C_8 (0.635e) that are taking part in intramolecular charge transfer is indicated in the NBO analysis. The LP(2)O_{16} participates as donor and the anti-bonding orbital for BD*(2)(C_{15}-O_{17}) acts as acceptor resulting in favorable resonance energy ($E^{(2)}$) ($O_{16} \rightarrow C_{15}$-$O_{17}$, 50.31 kcal mol^{-1}). Also BD(2)(C_2-C_3) participates as donor and the anti-bonding

Table 7 Second-order perturbation theory analysis (B3LYP/6-31G*) of Fock matrix in NBO basis threshold for compound **7a**.

Donor NBO (i)	Acceptor NBO (j)	$E^{(2)}$/kcal mol^{-1}
BD(2)C_1-C_6	BD*(2)(C_4-C_5)	23.20
BD(2)C_2-C_3	BD*(2)(C_1-C_6)	24.28
BD(2)C_2-C_3	BD*(2)(C_9-O_{11})	21.62
BD(2)C_4-C_5	BD*(2)(C_2-C_3)	23.97
BD(2)C_{14}-C_{20}	BD*(2)(C_{21}-C_{22})	18.86
BD(2)C_{14}-C_{20}	BD*(2)(C_{23}-C_{24})	21.75
BD(2)C_{21}-C_{22}	BD*(2)(C_{14}-C_{20})	22.42
BD(2)C_{23}-C_{24}	BD*(2)(C_{21}-C_{22})	20.88
LP(1)N_7	BD*(2)(C_1-C_6)	38.75
LP(1)N_7	BD*(2)(C_8-O_{10})	50.87
LP(2)O_{10}	BD*(1)(N_7-C_8)	30.21
LP(2)O_{16}	BD*(2)(C_{15}-O_{17})	50.31
LP(2)O_{17}	BD*(1)(C_{15}-C_{16})	32.54

BD*(2)(C_1-C_6) and BD*(2)(C_9-O_{11}) orbital act as acceptor. The resonance energies ($E^{(2)}$) for the transfer of electron density from BD(2)(C_2-C_3) of the isatin ring to the anti-bonding BD*(2)(C_1-C_6) and BD*(2)(C_9-O_{11}) orbitals of the isatin ring are 24.28 and 21.62, respectively. These values indicate large charge transfer from the bonding orbital for BD(2)(C_2-C_3) to the anti-bonding orbital for BD*(2)(C_1-C_6) [C_2-$C_3 \rightarrow C_1$-C_6].

2.4. Electronic Properties

Quantum chemical methods are important to obtain information about molecular structure and electrochemical behaviour. Figure 4 shows the results of the frontier molecular orbitals (FMO) analysis calculated for molecule **7a** with B3LYP/6-31G*. According to Fig. 4, charge transfer is taking place within the molecule. The HOMO and HOMO-1 orbitals are localized mainly on the isatin ring and phenyl ring whereas LUMO and LUMO+1 orbitals are localized mainly on the isatin ring. The calculated values are –8.99, –8.73, 1.36, 2.1 and 10.09 eV for E_{HOMO-1}, E_{HOMO}, $E_{LUMO,}$ E_{LUMO+1} and the HOMO–LUMO gap (ΔE), respectively. The energy of the HOMO is directly related to the

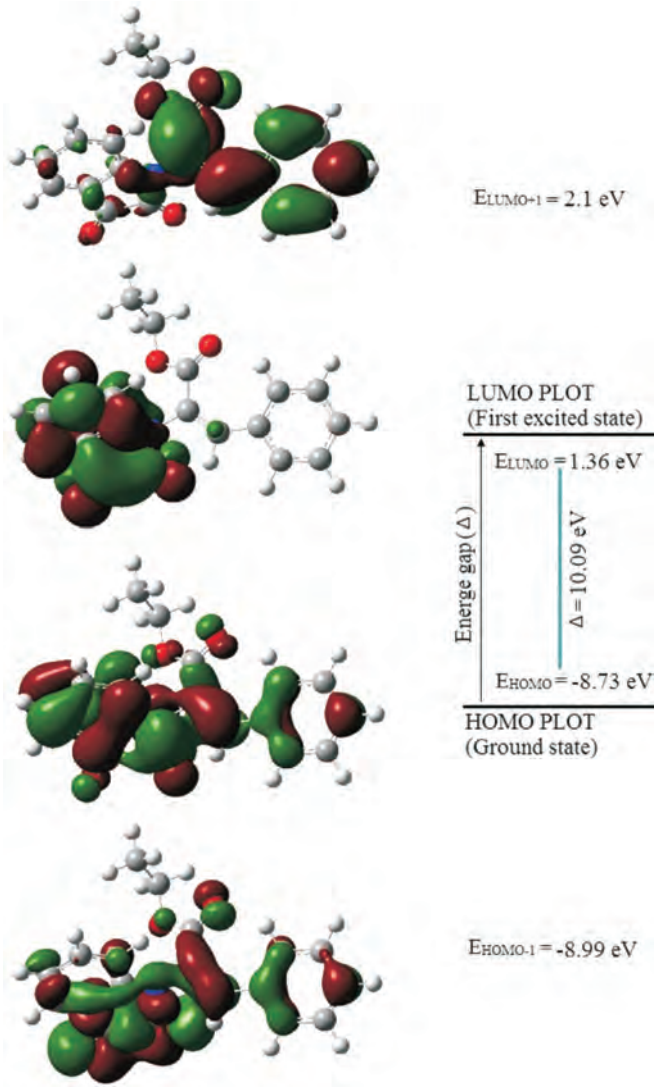

Figure 4 Calculated Frontier molecular orbitals of compound **7a** (Δ: energy gap between LUMO and HOMO - B3LYP/6-31G*).

ionization potential and the energy of the LUMO is directly related to the electron affinity. The HOMO–LUMO gap (ΔE), is 10.09 eV and such a large energy gap implies high stability for the molecule.[35–37] Also ionization potential (I), electron affinity (A), chemical hardness (η), electronic chemical potential (μ) and electrophilicity (ω) of molecule **7a** were calculated and are listed in Table 8.

Table 8 Calculated (B3LYP/6-31G*) HOMO, LUMO, energy gaps (HOMO–LUMO) and related molecular properties of molecule **7a**.

Property	Value
Energy (Hatree-Fock)	–1088.702
μ_D/Debye	4.942
E_{HOMO}/eV	–8.73
E_{LUMO}/eV	1.36
E_{HOMO-1}/eV	–8.99
E_{LUMO+1}/eV	2.1
Energy gap (E_g)/eV	10.09
Ionization potential ($I = -E_{HOMO}$)/eV	8.73
Electron affinity ($A = -E_{LUMO}$)/eV	–1.36
Chemical potential ($\mu = -(I + A)/2$)/eV	–3.68
Global hardness ($\eta = (I - A)/2$)/eV	5.04
Global electrophilicity ($\omega = \mu^2/2\eta$)/eV	1.34

3. Experimental

Chemicals used in this work were purchased from Aldrich and Merck chemical companies and used without purification. IR spectra were recorded on a mattson-1000 FT spectrometer using KBr pellets. ^{1}H and ^{13}C NMR spectra were measured for samples in $CDCl_3$ with a BRUKER DRX-250 AVANCE spectrometer at 250 and 62.5 MHz respectively, using Me_4Si as internal standard. Melting points were measured on an Electrothermal 9100 apparatus. Elemental analyses for C, H and N were performed using a Perkin-Elmer 2400 series analyzer.

3.1. General Procedure for the Synthesis 7a–g: (note 7f was only observed in trace amounts)

A solution of triphenylphosphine (1.0 mmol, 0.262 g) and isatin derivatives (1.0 mmol) in dry dichloromethane (10 mL) was placed in a three-necked flask in an ice-water bath. Then, a solution of acetylenic esters (1.0 mmol) in dry dichloromethane (4 mL) was added dropwise and stirred for 5 min. After 5 min, the mixture was cooled to room temperature and then stirred for an appropriate time (Table 1) until the reaction was completed as monitored by TLC (*n*-hexane/EtOAc; 2:1) analysis. The solvent was removed under reduced pressure and the residue was purified by column chromatography with silica gel 60 HF-254 using petroleum ether/EtOAc (10:2) as eluent. All the products were characterized by spectral data (IR, ^{1}H NMR and ^{13}C NMR). The physical and spectral data for the products are given below and the NMR and IR data are also presented with the supplementary material.

*Ethyl-(E)-2-(2,3-dioxo-2,3-dihydro-1*H*-indol-1-yl)-3-phenyl-2-propenoate* (**7a**)

Orange crystals (46 %).Mp 168–170 °C. R_f (EtOAc/ *n*-hexane: 1/2) = 0.34, IR (KBr): ν = 3061 (CH, arom), 2984 (CH, alipha), 1746, 1723, 1615 (3C=O), 1469 (C=C, alkene) cm^{-1}, ^{1}H NMR ($CDCl_3$) δ (ppm): 1.1 (t, 3H, ^{3}JHH = 7.0 Hz, CH_3), 4.2 (q, 2H, $^3J_{HH}$ = 7.0 Hz, OCH_2), 7.1–7.7 (m, 9H, arom), 5.3 (s, 1H, =CH). ^{13}C NMR ($CDCl_3$) δ (ppm): 14 (CH_3), 62.2 (OCH_2), 132.5 (=CH), 111.2, 118.2, 120, 122.5, 123.2, 124.4, 125, 128.3, 129.6, 129.8, 138.6, 141.2, 151.2 (12C of aromatic and =C-N), 158 (C=O of amide), 163 (C=O of ester), 182.4 (C=O of ketone); Anal. Calcd. for $C_{19}H_{15}O_4N$: C, 71.02, H, 4.70, N, 4.36; found C, 70.96, H, 4.81, N, 5.05.

*Ethyl-(Z)-2-(2,3-dioxo-2,3-dihydro-1*H*-indol-1-yl)-3-phenyl-2-propenoate* (**7b**).

Red crystals (54 %). Mp 168–170 °C. R_f (EtOAc/*n*-hexane: 1/2) = 0.33, IR (KBr): ν= 3091 (CH, arom), 2923 (CH, alipha), 1746, 1746, 1615 (3C=O), 1469 (C=C, alkene) cm^{-1}, ^{1}H NMR ($CDCl_3$) δ (ppm): 1.3 (t, 3H, $^3J_{HH}$ = 7.0, CH_3), 4.3 (q, 2H, $^3J_{HH}$ = 7.0 Hz, OCH_2), 6.6–8 (m, 9H, arom), 8.1 (s, 1H, = CH). ^{13}C NMR ($CDCl_3$) δ (ppm): 14.2 (CH_3), 62.3 (OCH2), 131.6 (= CH), 111.5, 118.2, 121.1, 124.4, 125.8, 128.2, 129.2, 129.8, 131.2, 135.8, 138.7, 142.6, 150.6 (12C of aromatic and =C-N), 158 (C=O of amide), 163.00 (C=O of ester), 181.9 (C=O) of ketone); Anal. Calcd. for $C_{19}H_{15}O_4N$: C, 71.02, H, 4.70, N, 4.36; found C, 71.00, H, 4.92, N, 5.12.

*Ethyl-2-(2,3-dioxo-2,3-dihydro-1*H*-indol-1-yl)-acrylate* (**7c**)

Orange solid (85 %). Mp 110 °C. R_f (EtOAc/ *n*-hexane: 1/2) = 0.35, IR (KBr): ν= 3092 (CH, arom), 2923 (CH, alipha), 1746, 1730, 1646 (3C=O), 1615 (C=C, alkene) cm^{-1},^{1}H NMR ($CDCl_3$) δ (ppm): 1.3 (t, 3H, $^3J_{HH}$ = 7.0 Hz, CH_3), 4.8 (q, 2H, $^3J_{HH}$ = 7.0 Hz, OCH_2), 6.7–7.7 (m, 4H, arom), 6.1, 7.3 (2s, 2H, ^3J = 0 Hz, = CH_2), ^{13}C NMR ($CDCl_3$) δ (ppm): 14.1(CH_3), 62.3 (OCH_2), 128.6 (=CH_2), 111.3, 118, 124.3, 125.6, 130.9, 132, 138.4 (6C of aromatic and =C-N), 161.6 (C=O of amide), 161.7 (C=O of ester), 183.4 (C=O of ketone); Anal. Calcd. for $C_{13}H_{11}O_4N$: C, 63.67, H, 5.52, N, 5.71; found C, 63.51, H, 5.74, N, 5.90.

*Methyl-2-(2,3-dioxo-2,3-dihydro-1*H*-indol-1-yl)-acrylate* (**7d**)

Viscouse yellow oil (80 %). R_f (EtOAc/ *n*-hexane: 1/2) = 0.36, IR (KBr): ν = 3084 (CH, arom), 2923 (CH, alipha), 1738, 1707, 1630 (3C=O), 1592 (C=C, alkene)cm^{-}, ^{1}H NMR ($CDCl_3$) δ (ppm): 4.2 (s, 3H, $^3J_{HH}$ = 0 Hz, CH_3), 7.5–7.7 (m, 4H, arom), 7.2,7.7 (2s, 2H, $^3J_{HH}$ = 0 Hz, =CH_2), ^{13}C NMR ($CDCl_3$) δ (ppm): 51(CH_3), 128.3 (=CH_2), 112, 125.7, 128.6, 132, 132.2, 133.4, 145 (6C of aromatic and =C-N), 159 (C=O of amide), 162 (C=O of ester), 181 (C=O of ketone); Anal. Calcd. for $C_{12}H_9O_4N$: C, 62.34, H, 3.92, N, 6.06; found C, 62.13, H, 3.85, N, 5.94.

*Ethyl-(Z)-2-(5-fluoro-2,3-dioxo-2,3-dihydro-1*H*-indol-1-yl)-3-phenyl -2-propenoate* (**7e**)

Red solid (90 %). Mp 132 °C. R_f (EtOAc/ *n*-hexane: 1/2) = 0.30, IR (KBr): ν= 3069 (CH, arom), 2953 (CH, alipha), 1748, 1730, 1623 (3C=O), 1492 (C=C, alkene) cm^{-1}, ^{1}H NMR ($CDCl_3$) δ (ppm): 1.3 (t, 3H, $^3J_{HH}$ = 7.0 Hz, CH_3), 4.3 (q, 2H, $^3J_{HH}$ = 7.0 Hz, OCH_2), 7.1–7.6 (m, 9H, arom), 8.1 (s, 1H, =CH), ^{13}C NMR ($CDCl_3$) δ (ppm): 14.2 (CH_3), 62.3 (OCH_2), 131.5 (=CH), 112.8, 118.2, 121.0, 125, 125.4, 128, 129, 129.2, 129.8, 131, 131.3, 142.7, 146.6 (12C of aromatic and =C-N), 162.8 (C=O of amide), 162.8 (C=O of ester), 181 (C=O of ketone); Anal. Calcd. for $C_{19}H_{14}O_4NF$: C, 67.25, H, 4.16, N, 4.13; found C, 67.31, H, 4.25, N, 4.08.

*Methyl-2-(5-fluoro-2,3-dioxo-2,3-dihydro-1*H*-indol-1-yl)-3-phenyl-2 -propenoate* (**7g**)

Yellow solid (95 %). Mp 135 °C. R_f (EtOAc/ *n*-hexane: 1/2) = 0.31, IR (KBr): ν = 3053 (CH, arom), 2961 (CH, alipha), 1738,1707, 1630 (3C=O), 1584 (C=C, alkene) cm^{-1}, ^{1}H NMR ($CDCl_3$) δ (ppm): 3.5 (s, 3H, $^3J_{HH}$ = 0 Hz, CH_3), 7.4–7.8 (m, 3H, arom), 7.5, 7.6 (d, 2H, $^3J_{HH}$ = 1.5 Hz, = CH_2), ^{13}C NMR ($CDCl_3$) δ (ppm): 52 (CH_3), 128.4 (=CH_2), 112, 131.9, 132.2, 132.3, 133.5, 142.4, 150 (6C of aromatic and =C-N), 158 (C=O of amide), 163.0 (C=O of ester), 181.9 (C=O of ketone); Anal. Calcd. for $C_{12}H_8O_4NF$: C, 57.83, H, 3.23, N, 5.62; found C, 57.93, H, 3.11, N, 5.49.

4. Computational Details

The *ab initio* molecular calculations were carried out using the Gaussian 98 software package[38] at the HF and DFT/B3LYP[39] levels of theory with the 6-31G* basis set. Also, geometry optimization and NBO analysis[40] in vacuum (gas phase) for molecules were performed. The Cartesian coordinates of the 3D structures for all these compounds are provided with the supplementary material. The ^{1}H and ^{13}C NMR chemical shifts of the compounds were calculated using the GIAO approach. The calculations also provide valuable information for exploring the thermodynamic parameters. We obtained the energy (ΔE), enthalpies (ΔH), Gibss free energy (ΔG), entropies (ΔS) and constant volume molar heat capacity (Cv) values of products.[41–43] Electronic properties such as energy of the highest occupied molecular orbital (E_{HOMO}), energy of the lowest unoccupied molecular orbital (E_{LUMO}), HOMO–LUMO energy gap (E_g), atomic charges and dipole moment (μ) were determined. The optimized molecular structure (Fig. 2), HOMO and LUMO surfaces were visualized using GaussView 03 program.[44]

5. Conclusions

We have described a convenient three-component route for the preparation of six novel electron-poor alkenes **7a–g**. The reactions were carried out in one-pot without separation and purification of the intermediates **3, 5** and **6**. The present procedure has many advantages such as good to high yields, environmentally friendly nature and fairly mild reaction conditions. In the present study also, ^{1}H and ^{13}C NMR chemical shifts were obtained using theoretical calculations. Good agreement between the experimental and calculated ^{1}H and ^{13}C NMR chemical shifts of compounds were obtained. The ^{13}C NMR correlation value (R^2) of molecule **7a** confirms this agreement. Thermodynamic analysis indicated that these compounds are stable in gas phase. According to the NBO analysis, the greatest resonance energy ($E^{(2)}$) was obtained for LP(1)N_7 that participates as electron donor and the anti-bonding BD*(2)(C_8-O_{10}) orbital as acceptor. This result shows that charge is transferred from N_{10} to C_{11}-O_{20} (N_{10}→ C_{11}-O_{20}). The FMO analysis suggests that charge transfer is taking place within the molecule and the HOMO is focused mainly on isatin ring and phenyl ring whereas the LUMO resides on the isatin ring. The HOMO–LUMO measured energy gap (E_g) for **7a** was 10.09 eV.

Supplementary material

The IR, MS and NMR spectra of these compounds are provided as supplementary material. The Cartesian coordinates of the optimized structures of these compounds are also provided with that.

Acknowledgements

We thank from research council of Young Researchers and Elite Club of Islamic Azad University, Gorgan Branch, Iran, for financial support.

References

1 M.A. De La Cruz, H. Shabany and D.C. Spilling, *Phosphorus, Sulfur Silicon Relat. Elem.*, 1999, **146**, 181–184.
2 H.D. Durst, D.K. Rohrbaugh and S. Munavalli, *Phosphorus, Sulfur Silicon Relat. Elem.*, 2009, **184**, 2902–2909.
3 G. Cera, P. Crispino, M. Magda Monari and M. Bandini, *Chem. Commun*., 2011, **47**, 7803–7805.
4 I. Yavari, N. Hazeri, M.T. Maghsoodlou and S.J. Souri, *Mol. Catal. A - Chem.*, 2007, **264**, 313–317.
5 A. Alizadeh, S. Rostamnia and L.G. Zhu, *Tetrahedron*, 2006, **62**, 5641–5644.
6 A. Shaabani, E. Soleimani and A. Maleki, *Tetrahedron Lett.*, 2006, **47**, 3031–3034.
7 A. Shaabani, M.B. Teimouri and H.R. Bijanzadeh, *Tetrahedron Lett.*, 2002, **43**, 9151–9154.
8 A. Shaabani, I. Yavari, M.B. Teimouri, A. Bazgir and H.R. Bijanzadeh, *Tetrahedron*, 2001, **57**, 1375–1378.
9 S.M. Habibi-Khorassani, M.T. Maghsoodlou, N. Hazeri, K. Bagherpour, M. Rostamizadeh and H. Najafi, *Phosphorus, Sulfur Silicon Relat. Elem.*, 2010, **186**, 1395–1403.
10 (a) A.A. Esmaeili, R. Hosseinabadi and M. Razi, *Phosphorus, Sulfur Silicon Relat. Elem.*, 2011, **186**, 2267–2273. b) D. Azarifar and D. Sheikh, *Synth. Commun*., 2013, **43**, 2517–2526.
11 U. Bora, A. Saikia and R.C. Boruah, *Org. Lett.*, 2003, **5**, 435–438. b) D. Azarifar, D. Sheikh, *Helv. Chim. Acta,* 2012, **95**, 1217–1225.
12 H.M.R. Hoffman and J. Rabe, *Helv. Chim. Acta*, 1984, **67**, 413–415.
13 F. Ameer, S.E. Drewes, N.D. Emslie, P.T. Kaye and R.L. Mann, *J. Chem. Soc. Perkin Trans. 1*, 1983, **28**, 2293–2295.
14 M. Paira, B. Banerjee, S. Jana, S.K. Mandal and S.C. Roy, *Tetrahedron Lett.*, 2007, **48**, 3205–3207.
15 H.M.R. Hoffmann and J. Rabe, *J. Org. Chem.*, 1985, **50**, 3849–3859.
16 E.K. Scott, B. Martin, T. Raj and K. Gall, *Polymer.*, 2009, **50**, 5549–5558.
17 L. Lienafa, S. Monge and J.J. Robin, *Eur. Polym. J.*, 2009, **45**, 1845–1850.
18 D. Baskaran, *Prog. Polym. Sci.*, 2003, **28**, 521–581.
19 L. Feng, Z. Zhang, F. Wang, T. Wang and S. Yang, *Fuel Processing Technol.*, 2014, **118**, 42–48.
20 H. Bakhshi, M.J. Zohuriaan-Mehr, H. Bouhendi and K. Kabiri, *Polymer Testing*, 2009, 28, 730–736.
21 C.J. Cramer, *Essentials of Computational Chemistry: Theories and Models*, Wiley, Chichester, 2002.
22 D. Avci and Y. Atalay, *Struct. Chem*., 2009, **20**, 185–201. b) R.B. Nazarski, *J. Phys. Org. Chem*., 2009, **22**, 834–844.

23 S.M. Shoaei, A.R. Kazemizadeh and A. Ramazani, *Chin. J. Struct. Chem*., 2011, **30**, 568–574.

24 E. Vessally, *Russ. J. Phys. Chem. A.*, 2011, **85**, 245–247.

25 H. Hopfl, B. Gomez and R. Martinez-Palou, *J. Mex. Chem. Soc.*, 2005, **49**, 307–311.

26 G.S. Suresh Kumar, A. Antony Muthu Prabu, S. Jegan Jenniefer, N. Bhuvanesh, P. Thomas Muthiah and S. Kumaresan, *J. Mol. Struct.*, 2013, **1047**, 109–120.

27 J. Casanovas, A.M. Namba, R. da Silva and C. Aleman, *Bioorg. Chem.*, 2005, **33**, 484–492.

28 H. Khanmohammadi and M. Erfantalab, *Spectrochim. Acta A,* 2010, **75**, 127–133.

29 H. Khanmohammadi, H. Keypour, M. SalehiFard and M.H. Abnosi, *J. Incl. Phenom. Macro.*, 2009, **63**, 97–108.

30 I.Yavari and M.T. Maghsoodlou, *Tetrahedron Lett.*, 1998, **30**, 4579–4580.

31 A. Ramazani, P. Pakravan, M. Bandpey, N. Noshiranzadeh and A. Souldozi, *Phosphorus, Sulfur, and Silicon*, 2007, **182**,1633–1640.

32 A. Ramazani, A. Safari and N. Noshiranzadeh, *Int. J. Sci. Technol.*, 2009, **16**, 7–11.

33 R.P. Gangadharana and S.S. Krishnanb, *Act. Phys. Polon. A*, 2014, **125**, 18–22.

34 B.D. Joshi, P. Tandon and S. Jain, *Himalayan Phys.*, 2012, **3**, 44–49.

35 A.E. Reed, L.A. Curtiss and F. Weinhold, *Chem. Rev.,* 1988, **88**, 899–926.

36 P. Politzer and D.G. Truhlar, *Chemical Applications of Atomic and Molecular Electrostatic Potentials*, Plenum Press, New York, 1981.

37 P.K. Chattaraj, U. Sarkar and D.R. Roy, *Chem. Rev.,* 2006, **106**, 2065–2091.

38 M.J.Frisch, G.W. Trucks, H.B. Schlegel, G.E. Scuseria, M.A. Robb, J.R. Cheeseman, V.G. Zakrzewski, J.A. Montgomery, R.E. Stratmann, J.C. Burant, S. Dapprich, J.M. Millam, A.D. Daniels, K.N. Kudin, M.C. Strain, O. Farkas, J. Tomasi, V. Barone, M Cossi, R, Cammi, B Mennucci, C. Pomelli, C. Adamo, S. Clifford, J. Ochterski, G.A. Petersson, P.Y. Ayala, Q, Cui, K. Morokuma, D.K. Malick, A.D. Rabuck, K. Raghavachari, J.B. Raghavachari, J. Cioslowski, J.V. Ortiz, A.G. Baboul, B.B. Stefanov, G. Liu, A. Liashenko, P. Piskorz, I. Komaromi, R. Gomperts, R.L. Martin, D.J. Fox, T. Keith, M.A. Laham, C.Y. Peng, A. Nanayakkara, C. Gonzalez, M. Challacombe, P.M.W. Gill, B. Johnson, W. Chen, M.W. Wong, J.L. Andres, C. Gonzalez, M.H. Gordon, E.S. Replogle and J.A. Pople, Gaussian 98 Revision A.7, Gaussian, Inc., Pittsburgh PA, 1998.

39 a) A.D. Becke. *J. Chem. Phys.*, 1993, **98**, 5648–5652. b) C. Lee. W. Yang and R.G. Parr, *Phys. Rev. B.,* 1998, **37**, 785–789.

40 a) M. Monajjemi, M. Sheikhi, M. Mahmodi Hashemi, F. Molaamin and R. Zhiani. *Inter. J. Phys. Sci.*, 2012, **7**, 2010–2031. b) S.A. Seyed Katouli, M. Sheikhi, D. Sheikh and S.F. Tayyari, *Orient J. Chem.,* 2013, **29**, 1121–1128.

41 M. Monajjemi, S. Afsharnezhad, M.R. Jaafari, T. Abdolahi, A. Nikosade and H. Monajjemi. *Phys. Chem. Liquids*, 2011, **49**, 318–336.

42 a) M. Monajjemi, L. Mahdavian, F. Mollaamin and B. Honarparvar. *Fullerenes, Nanotubes. Carbon Nano-structures*, 2010, **18**, 45–55. b) L. Shiri, D. Sheikh, A.R. Faraji, M. Sheikhi and S.A. Seyed Katouli, *Lett. Org. Chem.*, 2014, **11**, 18–28.

43 A.R. Soltani, M.T. Baei, M. Mirarab, M. Sheikhi and E.Tazikeh Lemeski, *J. Phys. Chem. Solids.*, 2014, **75**, 1099–1105.

44 A. Frisch, A.B. Nielson and A.J. Holder, *GAUSSVIEW User Manual*, Gaussian Inc., Pittsburgh, PA, 2000.